FULL PAPER

Direct Synthesis of Spin-Crossover Complexes: a New Iron-Triazolic Structure Unexpectedly Revealed

Valerii Y. Sirenko,[a] Olesia I. Kucheriv,[a,b] Aurelian Rotaru,[c] Igor O. Fritsky,[a,b] and Il'ya A. Gural'skiy*[a,b]

Abstract: Spin-crossover complexes form one of the biggest families of switchable compounds. Here we show a new way to obtain spin-crossover materials by direct synthesis from metallic iron. Four complexes of Fe^{II} with 4-R-1,2,4-triazoles have been synthesized by a direct metal oxidation: $[Fe(NH_2trz)_3]SO_4$, $[Fe(NH_2trz)_3](BF_4)_2$ and two polymorphs of $[Fe(Htrz)_2(trz)]BF_4$. Surprisingly high quality of PXRD pattern of $[Fe(NH_2trz)_3]SO_4$ allowed to perform Rietveld refinement and obtain reliable crystal structure of the latter. All compounds have been studied by magnetic susceptibility measurements, optical reflectivity, differential scanning calorimetry and Raman spectroscopy. Importantly, spin-crossover characteristics of the complexes obtained by this unusual method are preserved, thus revealing a new effective approach of "direct synthesis" towards switchable coordination compounds.

Introduction

Spin crossover (SCO) is a spectacular ability of some 3*d* metal complexes to switch between two different spin states, which can be triggered by the influence of such external stimuli as temperature, pressure, light irradiation, magnetic field or adsorption of different chemical compounds.[1] SCO in iron(II) occurs between the diamagnetic (S = 0) low-spin (LS) state (with all *d*-electrons coupled – $t_{2g}^6e_g^0$) and paramagnetic (S = 2) high-spin (HS) state (with four unpaired *d*-electrons $t_{2g}^4e_g^2$). Along with the change of electronic configuration, the whole set of physical properties changes to some extent during the spin transition. The most notable changes concern magnetic, optical,[2] mechanical[3] and electric[4,5] properties. As a result, SCO complexes found their numerous applications as actuators,[3] chemical sensors,[6,7] switchable catalysts,[8] microwave radiation switches,[9] memory displays,[10] microthermometers,[11] nanoelectronic devices,[12] etc. Additionally, inclusion of different molecules in frameworks of SCO compounds leads to a shift of SCO characteristics such as a spin transition temperature and width of hysteresis.[6]

[a] Mr. V.Y. Sirenko, Mrs. O.I. Kucheriv, Dr. I.A. Gural'skiy, Prof. Dr. I.O. Fritsky
Department of Chemistry, Taras Shevchenko National University of Kyiv, Volodymyrska St. 64, Kyiv 01601, Ukraine
E-mail: illia.guralskyi@univ.kiev.ua
http://physchem.univ.kiev.ua/guralskyi
[b] Mrs. O.I. Kucheriv, Dr. I.A. Gural'skiy, Prof. Dr. I.O. Fritsky
UkrOrgSyntez Ltd,
Chervonotkatska St. 67, Kyiv 02094, Ukraine
[c] Dr. A. Rotaru
Faculty of Electrical Engineering and Computer Science, Stefan cel Mare University, Universității St. 13, Suceava 720229, Romania

Supporting information for this article is given via a link at the end of the document.

Numerous ways to synthesize SCO complexes have been offered for today, for example, solution state chemistry, mechanochemistry,[13] solvatothermal[14] and hydrothermal[15] syntheses, as well as more exotic approaches such as thermolysis of spin-crossover inactive complexes.[16]

"Direct synthesis" is a one-step synthesis of metal complexes starting from zero-valent metals or their oxides.[17] This approach attracts attention due to unusual experimental technique, less synthetic time, low cost, and convenient control over the whole process.[18] First report of obtaining new compounds from zero-valent metals with assistance of electric current dates back to 19th century.[19] Later there were reports of possibility to synthesize new coordination compounds from pure metals in gaseous phase,[20] in solutions in the presence of oxidants, as well as mechanochemically.[21] Additionally, almost all types of coordination compounds can be obtained by direct synthesis: molecular and π-complexes,[22] metal chelates,[23] dinuclear and polynuclear structures,[24] etc. For example, direct synthesis was successfully implemented for obtaining N-heterocyclic carbenes complexes of non-noble metals from commercially available metal powders, while conventional synthesis of these complexes is a highly complicated task.[25] Additionally, by means of direct synthesis, it is possible to obtain dialkylgermanes from germanium, which can be used as precursors for photoconducting polymers and photoresists.[26] Moreover, direct synthesis is widely used for obtaining classical commercial reagents. For example, there is a well-known reaction of magnesium with alkyl and aryl halides in ether to produce the Grignard reagents.[27] As well, direct synthesis allows to avoid complicated steps of preparing salts[28,29] that sometimes can be crucial in case of iron(II) compounds. For example, such salts as $Fe(OTs)_2$ (OTs = p-toluenesulfonate)[30] or $Fe((R\text{ or }S)\text{-CSA})_2$ (CSA = camphorsulfonate)[31] are not commercially available. In such cases, direct synthesis approach becomes very useful because it does not require salt synthesis step in obtaining SCO complexes.

Herein, we present the new way to obtain SCO complexes of triazole family using direct synthesis. In our study we chose Fe^{II} complexes with 4-R-1,2,4-triazoles that belong to one of the biggest families of SCO materials.[32] These complexes became well known due to the simplicity of their synthesis, practically attractive transition temperatures and variety of functional forms that can be achieved. Due to these reasons triazolic complexes have found their numerous applications: in the production of memory devices,[10] thermochromic pigments, in chemical sensors[33] etc.

For our experiments we selected four well-known SCO complexes: $[Fe(NH_2trz)_3]SO_4$ (**1**), $[Fe(NH_2trz)_3](BF_4)_2$ (**2**) and two forms of $[Fe(Htrz)_2(trz)]BF_4$ (**3,4**) (where NH_2trz = 4-amino-1,2,4-triazole, Htrz = 4-H-1,2,4-triazole, trz^- = 1,2,4-triazolato anion). According to the literature, the spin transition in dehydrated $[Fe(NH_2trz)_3]SO_4$ occurs at $T_{1/2}\uparrow$ = 355 K and at $T_{1/2}\downarrow$ = 323 K (ΔT

= 32 K).[34] For $[Fe(Htrz)_2(trz)]BF_4$ two polymorphs with different spin transition temperatures, abruptness, hysteresis width are obtained.[35] For the first polymorph spin transition occurs at $T_{1/2}\uparrow$ = 385 K and $T_{1/2}\downarrow$= 345 K with ΔT = 40 K. At the same time, in the second polymorph spin transition is less abrupt and has hysteresis of ΔT = 19 K. SCO for second polymorph occurs at $T_{1/2}\uparrow$ = 344 K and $T_{1/2}\downarrow$= 325 K. To the best of our knowledge, three examples of $[Fe(NH_2trz)_3](BF_4)_2$ with different SCO characteristics are described.[36–40] Unfortunately, there is no structural investigation for these examples and for this reason it is not allow us to assign these examples as different polymorph of $[Fe(NH_2trz)_3](BF_4)_2$. For $[Fe(NH_2trz)_3](BF_4)_2{\cdot}H_2O$, obtained from methanol, gradual spin transition is observed.[37,40] Mössbauer spectroscopy measurements of this example showed that at 77 K all SCO centers are in LS state and at 293 K there is a mixture of LS and HS states. In other studies second example of $[Fe(NH_2trz)_3](BF_4)_2$ was described with the hysteresis width of 6 K.[38,39] The spin transition in this complex occurs in the vicinity of room temperature with $T_{1/2}\uparrow$ = 278 K and $T_{1/2}\downarrow$ = 272 K. In the third example of $[Fe(NH_2trz)_3](BF_4)_2$ SCO occurs at $T_{1/2}\uparrow$ = 335 K and at $T_{1/2}\downarrow$ =307.[34,36]

All four compounds obtained by “direct synthesis” display a SCO behavior that proves the efficiency of this approach towards obtaining spin-transition complexes. Notably, surprisingly high quality of PXRD pattern of **1** allowed to perform the Rietveld refinement and to obtain a new crystal structure of Fe^{II} triazolic complex.

Results and Discussion

Direct synthesis

The oxidative dissolution of transition metals in the liquid phase takes place according to the reaction given in Scheme 1. Direct synthesis can be carried out in both water or organic solvents. To implement direct synthesis approach for SCO compounds we used iron powder, 4-R-1,2,4-triazole (R = NH_2 (**1**, **2**), H (**3**, **4**)) and alkali/ammonia salts which included the corresponding anion ($(NH_4)_2SO_4$ for **1**, $NaBF_4$ for **2–4**). The reaction took place in a slightly acidic environment (reached with corresponding acids) in order to facilitate the dissolution of iron. The mixture was left to stir for about one week; during the flow of the reaction the formation of SCO complex was observed. After that, the reaction mixture was easily purified from the leftovers of iron with a NdFeB magnet. The precipitate was separated from solvent by centrifugation.

$$2Fe^0 + 4X^- + 6Rtrz + O_2 + 4H^+ + 2nSolv \rightarrow 2[Fe^{2+}(Rtrz)_3]X_2{\cdot}nSolv + 2H_2O$$

Scheme 1. Scheme of direct synthesis of Fe-triazole complexes. X is the anion, Rtrz is the 4-R-1,2,4-triazole, Solv – solvent.

PXRD patterns for **3** and **4** obtained by direct synthesis and corresponding complexes prepared by conventional method[35] showed the same PXRD patterns. At the same time, **2** showed different PXRD pattern in comparison with $[Fe(NH_2trz)_3](BF_4)_2$, obtained from ethanol by conventional method.

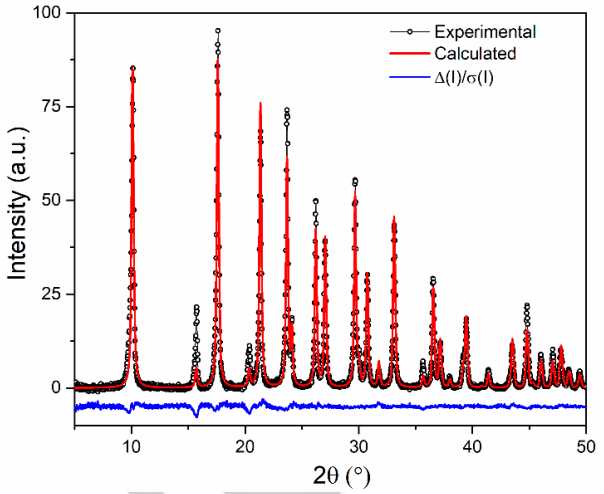

Figure 1. Experimental (black circles) and calculated (red line) diffraction patterns of **1**. The difference pattern divided by signal to noise ratio is shown as a blue line.

Crystal structure of $[Fe(NH_2trz)_3]SO_4$

Despite the high popularity of SCO complexes, which belong to 1,2,4-triazole family, a serious issue is caused by a low degree of their crystallinity. To the best of our knowledge, there are only three crystal structures of triazole complexes known for today: two found for single crystals[41,42] and one refined for powder samples[43]. In 2011, Grosjean et al. performed first single-crystal X-ray diffraction analysis of the Fe-triazolic complex $[Fe(NH_2trz)_3]NO_3{\cdot}2H_2O$.[41] This complex crystalizes in $P\bar{1}$ space group. Fe atoms in this structure are connected through triazole ligands creating 1D infinite $[Fe(NH_2trz)_3]_\infty$ chains that propagate along the *a* direction.

Table 1. Crystal unit cell and Rietveld refinement data obtained for **1**

Temperature [K]	293	Wavelength, $K_\alpha1$, $K_\alpha2$ [Å]	1.54051, 1.54433
Crystal system	hexagonal	2Θ angular range [°]	5-50
Space group	$P6_3/m$	R_{wp} [%]	14.34 %
Cell parameters	a = b = 10.0742(23) Å c = 7.3823(5) Å α = β = 90 ° γ = 120 °	R_p [%]	10.57%
		Density (calculated) [g/cm^3]	2.06848
Z	2	Volume [Å^3]	648.85(21)

* The HS powder diffractogram of **1** was not obtained due to limitations of available setup.

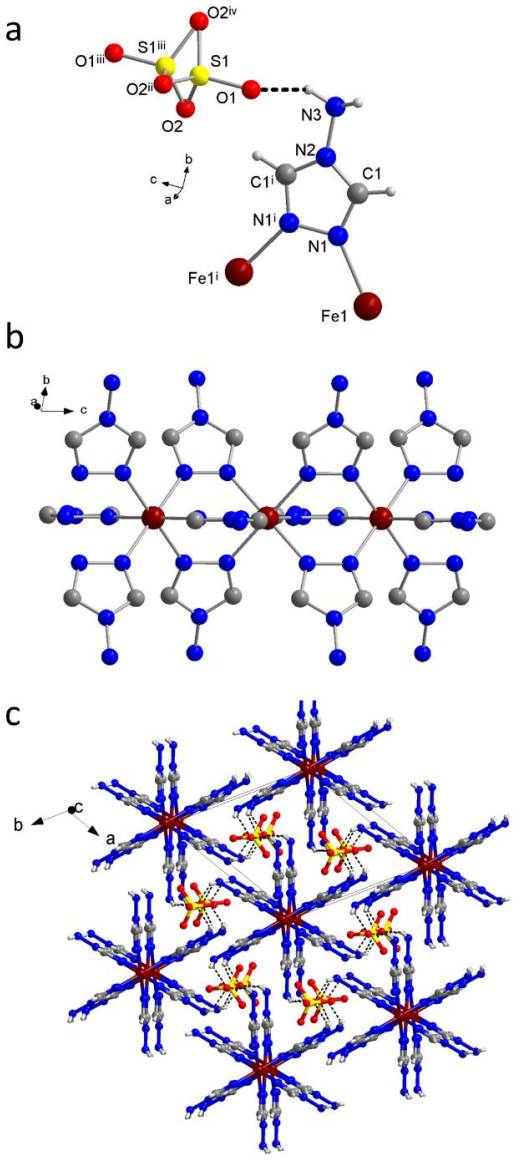

Figure 2. (a) A fragment of the molecular structure of **1** with atom labelling scheme. Symmetry codes: (i) x, y, 0.5-z; (ii) 1-y, x-y, -0.5-z; (iii) x, y, -0.5-z; (iv) 1+y-x, 1-x, z. (b) A view of 1D chains that propagate along the *c* axis in the crystal structure of **1**. (c) General view of the chains within the crystal packing along the *c* axis.

Anions and guest water molecules are located in the cavities among the chains, participate in the crystal cohesion and support intermolecular interaction through hydrogen bonding.

The first attempt to provide a crystal structure of "Fe(R-trz)$_3$A$_n$ family" was made by Urakawa at al. in 2010 by performing Rietveld refinement of PXRD pattern of [Fe(Htrz)$_2$(trz)]BF$_4$ complex.[35,44] However, this crystal structure was re-investigated in 2012 by Grosjean et al. by Rietveld refinement. It was reported to crystalize in *Pnma* space group[43]. This complex showed a similar 1D polymeric nature.

In 2017, Triki et al. proposed an approach to enhance the structure rigidity by implementation of some unusual building blocks into triazolic structure: rigid aryl groups with an alkyl spacer, coupled with more sophisticated anions such as polycyanometallates or organic cyanocarbanions.[42]

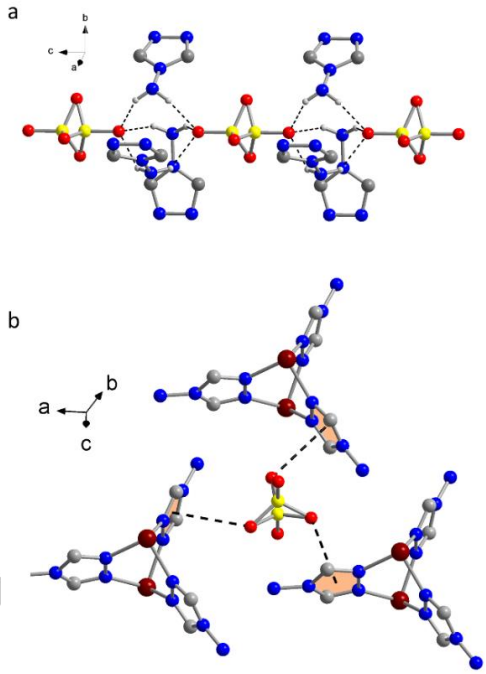

Figure 3. (a) A fragment of the molecular structure of **1** showing intermolecular hydrogen bonding contacts. (b) Demonstration of π···anion interactions in the crystal structure of **1**.

Based on this approach, the high quality single crystals of new triazolic compound with general formula [Fe(*bntrz*)$_3$][Pt(CN)$_4$]·H$_2$O (*bntrz* = 4-benzyl-4H-1,2,4-triazole) have been obtained and fully characterized by means of magnetic and single crystal investigations. At the same time, taking into account, that there are more than 50 iron(II)-triazolic SCO complexes known for today,[45] but only three of them were structurally characterized, it is still impossible to perform any reasonable structure-property correlations for such a big class of SCO complexes.

In our study, the powders of SCO complexes obtained by direct synthesis approach were characterized by PXRD. While **2–4** demonstrated poor diffraction patters (Figures S1–S3, ESI), which is typical for this class of complexes, **1** surprisingly showed a high degree of crystallinity and well resolved peaks on PXRD pattern, which was suitable for Rietveld refinement (Figure 1).

According to the simulated annealing, **1** crystalizes in the hexagonal *P*6$_3$/*m* space group with two formula units per cell. In this case, the high hexagonal symmetry of **1** favored the possibility to perform Rietveld refinement of PXRD pattern. Selected crystallographic data are summarized in Table 1. The Fe^{II} ions are located on the 6$_3$ screw axis and have an octahedral [FeN$_6$] environment created by N atoms of six 4-NH$_2$-1,2,4-triazole molecules (Figure 2a).

The coordination network is further connected by 4-NH$_2$-1,2,4-triazole molecules which act in μ$_2$-bridging mode creating 1D polymeric chains that propagate along the *c* axis (Figure 2b).

Each {[Fe(NH$_2$trz)$_3$]SO$_4$}$_\infty$ chain is surrounded by six identical chains in hexagonal manner with [Fe–Fe] = *a* = *b* = 10.0742(23) Å, angle Fe–Fe–Fe = 60° as shown in Figure 2c. From peak

broadening the chain length for **1** can be estimated approximately as ~180 Fe atoms.

No water or any other solvent molecules were found within the structure, additionally, structure analysis revealed that there are no solvent available voids.

Sulfate anions, which are disordered between two positions, are located in the voids between polymeric chains and interact with them via hydrogen bonding N–H···O = 1.939 Å, N···O = 2.660 Å (Figure 3a), providing a 3D supramolecular connectivity of the system. In addition, the structure is stabilized by anion···π interactions with a π-amphoteric 1,2,4-triazole ring (Figure 3b). As was previously shown, coordination of transition metal can significantly affect the ligand affinity in anion-π interactions.[46] In this case each sulfate anion interacts with triazole rings of three different chains (O2···centroid = 3.190 Å) providing additional rigidity of the structure. The O2 atom of sulfate anion is located practically above the centroids of triazole rings (angle of the O···π contact with aromatic plane is 85.17°) indicating a directional interaction. Similar 1,2,4-triazole·anion interactions were reported with BF_4^-, ClO_4^-, PF_6^- and $NCSe^-$ anions.[47,48]

It is worth noting, that crystallinity of the sample and thus the quality of PXRD pattern of **1** does not depend on synthetic approach that was applied. After receiving a PXRD pattern of very good quality for **1**, which was obtained by a direct synthesis approach, we measured a PXRD for $[Fe(NH_2trz)_3]SO_4$ sample, obtained by conventional method and it showed a similar degree of crystallinity (Figure S4, ESI). Thus, it is not the synthesis procedure, but the nature of the complex, which is responsible for high crystallinity and consequently high quality of PXRD patterns. Additionally, **3** and **4** obtained by direct synthesis and corresponding complexes prepared by conventional method showed the same PXRD patterns, however their SCO behavior is different. Here it is worth nothing, that very small differences in structure, that cannot be seen purely on PXRD, can drastically affect the SCO behavior and are well known in polymorphs.[49] At the same time, **2** showed different PXRD pattern in comparison with $[Fe(NH_2trz)_3](BF_4)_2$, obtained from ethanol by conventional method. This fact shows that direct synthesis approach can be applied for preparation of different modifications of one SCO Fe^{II} 1,2,4-triazolic complex.

Magnetic Properties

Measuring the magnetic susceptibility χ as a function of temperature is a standard method to study SCO systems because the change in the number of unpaired electrons between two spin states is reflected in a drastic change of the χ value.[1]

The transition phenomenon between the HS and LS states for the samples of **1–4** was monitored at 1000 Oe in the temperature range 70−400 K. The SCO behavior of **1–4** obtained by direct synthesis as a function of temperature is shown in Figure 4. Classic abrupt one-step hysteretic SCO takes place in complexes **1**, **3**, **4**. Gradual spin transition was observed for **2**. It was found that $T_{1/2}\uparrow$ and $T_{1/2}\downarrow$ for all complexes do not change in subsequent thermal cycles. The magnetic measurements of **1** revealed that at room temperature when the complex is in the LS state its $\chi_M T$ is 0.42 cm^3 K mol^{-1}. Upon heating transition from the LS to the HS takes place at $T_{1/2}\uparrow$ = 345 K. In cooling mode, the transition back to the LS state occurs at $T_{1/2}\downarrow$ = 330 K with hysteresis width ΔT = 15 K. At 400 K, $\chi_M T$ of **1** is equal to 3.41 cm^3 K mol^{-1}, which is expected for HS iron (II) compound. SCO in **2** represents a

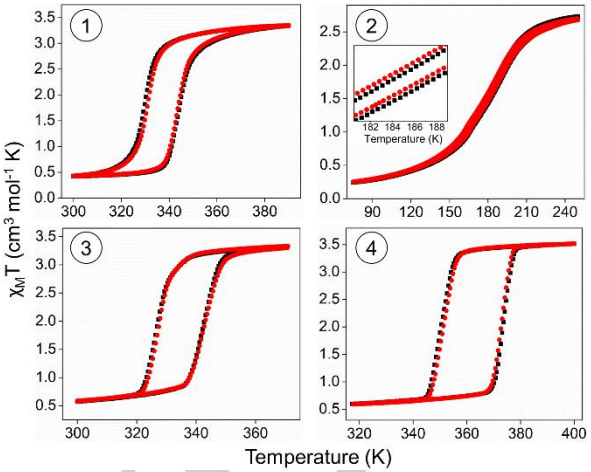

Figure 4. Magnetic properties of **1 – 4** shown in $\chi_M T$ vs. T plot. The curves were recorded in both heating and cooling modes with the scan rate of 3 K min^{-1}. 1st cycle – black squares, 2nd cycle – red circles.

gradual LS → HS transition with $T_{1/2}\uparrow$ = 180 K in heating mode. The similar character of curve is observed in cooling mode with $T_{1/2}\downarrow$ = 177 K and resulting in a small hysteresis width of ΔT = 3 K. The $\chi_M T$ for compound **2** in the LS form at 75 K equals 0.25 cm^3 K mol^{-1} and for the HS form at 250 K is 2.73 cm^3 K^1 mol^{-1}. The spin crossover for **2** is very gradual, that is why even at these temperatures the transition is not complete (minor low-spin residues at 250 K and high-spin residues at 70 K). Magnetic measurements confirm that compounds **3** and **4** are two modifications of $[Fe(Htrz)_2(trz)]BF_4$ obtained from different solvents.[35] The transition temperatures and hysteresis widths are notably different for these complexes. For **3** the spin transition occurs at $T_{1/2}\uparrow$ = 343 K in heating mode, while for compound **4** the LS → HS transition temperature is notably shifted to higher temperatures and takes place at $T_{1/2}\uparrow$ = 374 K. The same trend is observed in cooling mode, for **3** transition occurs at $T_{1/2}\downarrow$ = 328 K and for **4** at $T_{1/2}\downarrow$ = 351 K. The hysteresis width is also different for these compounds and are estimated as ΔT = 15 K for **3**, and ΔT = 23 K for **4**. The $\chi_M T$ values for LS forms of these complexes are 0.57 and 0.56 cm^3 K^1 mol^{-1} of **3** and **4**, respectively. For the HS forms of iron(II) the corresponding values are 3.3 cm^3 K mol^{-1} (at 365 K) for **3** and 3.5 cm^3 K^1 mol^{-1} (at 400 K) for **4**. Comparing with the transition temperatures mentioned in introduction part the transition temperature for complexes obtained by direct synthesis is slightly different but are still within expected range.

Optical reflectivity

Since the SCO is accompanied by a drastic change of color, there is a possibility additionally to follow spin transition properties by optical reflectivity.

Two thermal cycles of optical reflectivity measurements for **1–4** were performed after preliminary heating of the complexes that precluded influence of solvent molecules on spin transition curve (Figure S5, ESI).

The transition temperature are $T_{1/2}\uparrow$ = 347 K and $T_{1/2}\downarrow$ = 335 K (ΔT = 12 K) for **1**, $T_{1/2}\uparrow$ = 199 and $T_{1/2}\downarrow$ = 195 K (ΔT = 4 K) for **2**, $T_{1/2}\uparrow$ $T_{1/2}\uparrow$ = 325 K and $T_{1/2}\downarrow$ = 312 K (ΔT = 13 K) for **3**, $T_{1/2}\uparrow$ = 380 K and $T_{1/2}\downarrow$ = 357 K (ΔT = 23 K) for **4**. Optical reflectivity measurements agreement with magnetic measurements.

Table 2. Spin transition characteristics of **1**, **2** and **4** obtained from DSC measurements. Corresponding characteristics are also mentioned for some well-known complexes of this family for comparison.

Sample	№	$T_{1/2}\downarrow$ (K)	$T_{1/2}\uparrow$ (K)	$\Delta T_{1/2}$(K)	Δ H ↑ kJ mol^{-1}	Δ H ↓ kJ mol^{-1}	Δ S ↑ J mol^{-1} K^{-1}	Δ S ↓ J mol^{-1} K^{-1}
$[Fe(NH_2trz)_3]SO_4$	**1**	331	347	16	18.1	−15.0	52.1	−45.4
$[Fe(Htrz)_2(trz)]BF_4$	**3**	332	358	26	25.2	−23.7	70.4	−71.3
$[Fe(Htrz)_2(trz)]BF_4$	**4**	330	351	21	23.7	−23.4	67.5	−70.8
$[Fe(NH_2trz)_3]Br_2$[50]	–	318	328	10	22.3		67.6	
$[Fe(Htrz)_2(trz)]BF_4$ (**Ia**)[34]	–	345	385	40	27.8		75	
$[Fe(Htrz)_2(trz)]BF_4$ (**Ib**)[34]	–	323	343	20	22.5		77	
$[Fe(NH_2trz)_3](ClO_4)_2$[50]	–	165	165	0	4.4		30	

A slight difference in spin transition temperatures is caused by some thermalization aspects and different measurement rates during the experiment.

Differential Scanning Calorimetry Measurements

Differential scanning calorimetry (DSC) is a very sensitive and powerful tool to detect and study phase transition in SCO materials, in particular systems of Fe(II), where the primary driving force governing the spin conversion is the increase of entropy arising from differences in spin multiplicity and states between LS and HS forms. DSC measurements for compounds **1**, **3**, **4** were carried out at the scan rate of 10 K min^{-1} in heating and cooling modes. Due to very gradual manner of the spin transition in **2**, no notable bands were observed for this complex during DSC measurements.

The DSC curves of compounds **1**, **3**, **4** are given in Figure 5, the enthalpy and entropy values for SCO in all complexes are summarized in Table 2. As expected, compound **1** shows one endothermic peak in heating mode at $T_{1/2}\uparrow$ = 347 K (ΔH = 18.1 kJ mol^{-1}, ΔS = 52.1 J mol^{-1} K^{-1}) and one exothermic peak in cooling mode at $T_{1/2}\downarrow$ = 331 K (ΔH = −15.0 kJ mol^{-1}, ΔS = −45.4 J mol^{-1} K^{-1}).

Compound **3** shows two-step transition both in heating and cooling modes. In heating mode, the transition is observed at $T_{1/2}\uparrow$ = 351 K (ΔH = 25.2 kJ mol^{-1}, ΔS = 70.4 J mol^{-1} K^{-1}). In cooling mode, the HS → LS transition of **3** can be found at $T_{1/2}\downarrow$ = 330 K (ΔH = −23.7 kJ mol^{-1}, ΔS = −70.8 J mol^{-1} K^{-1}). For **4** two-step transition was observed in cooling and heating modes. In heating mode, it was observed at $T_{1/2}\uparrow$ = 358 K (ΔH = 23.7 kJ mol^{-1}, ΔS = 67.5 J mol^{-1} K^{-1}) and in cooling mode at $T_{1/2}\downarrow$= 332 K (ΔH = −23.4 kJ mol^{-1}, ΔS = −70.8 J mol^{-1} K^{-1}).

As magnetic and optical measurements did not show the two-step transition for these complexes, the double peak on DSC curve may indicate the presence of some hidden phase transition around the temperatures of SCO.

The transition temperatures found in DSC measurements are in good correlation with those found in magnetic and optical experiments.

Raman spectroscopy

Raman spectra were acquired for the solvent free bulk powders of **1–4** (Figure 6). For **1**, **3**, **4** complexes Raman spectra were recorded at different temperatures to show the change of vibration bands associated with SCO. At the same time, Raman spectrum was acquired only for the HS form of **2**, due to a very low temperature of the spin transition which could not be reached with the available setup. Raman spectra of the complexes **1, 3, 4** in both HS

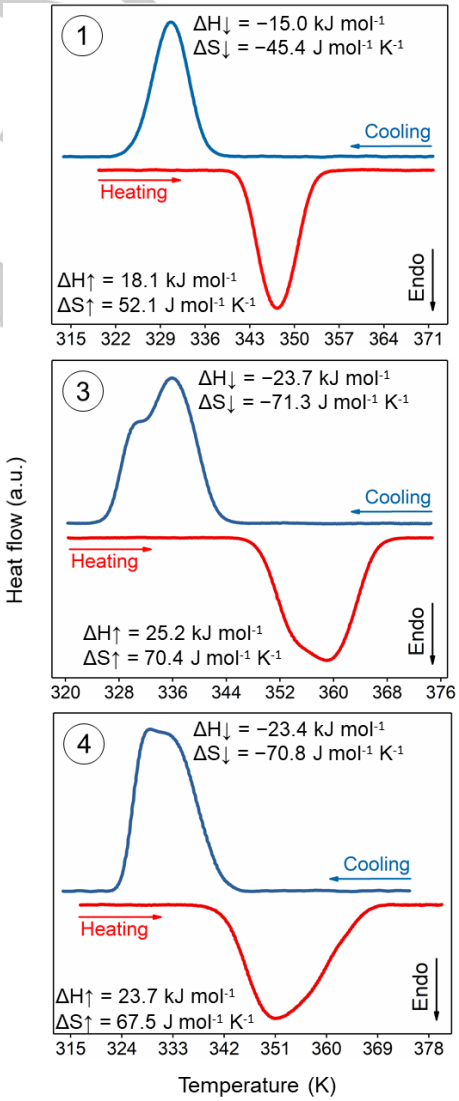

Figure 5. DSC measurements of **1**, **3**, **4** demonstrating endothermic and exothermic anomalies upon spin transition. All curves were recorded at the rate 10 K min^{-1}.

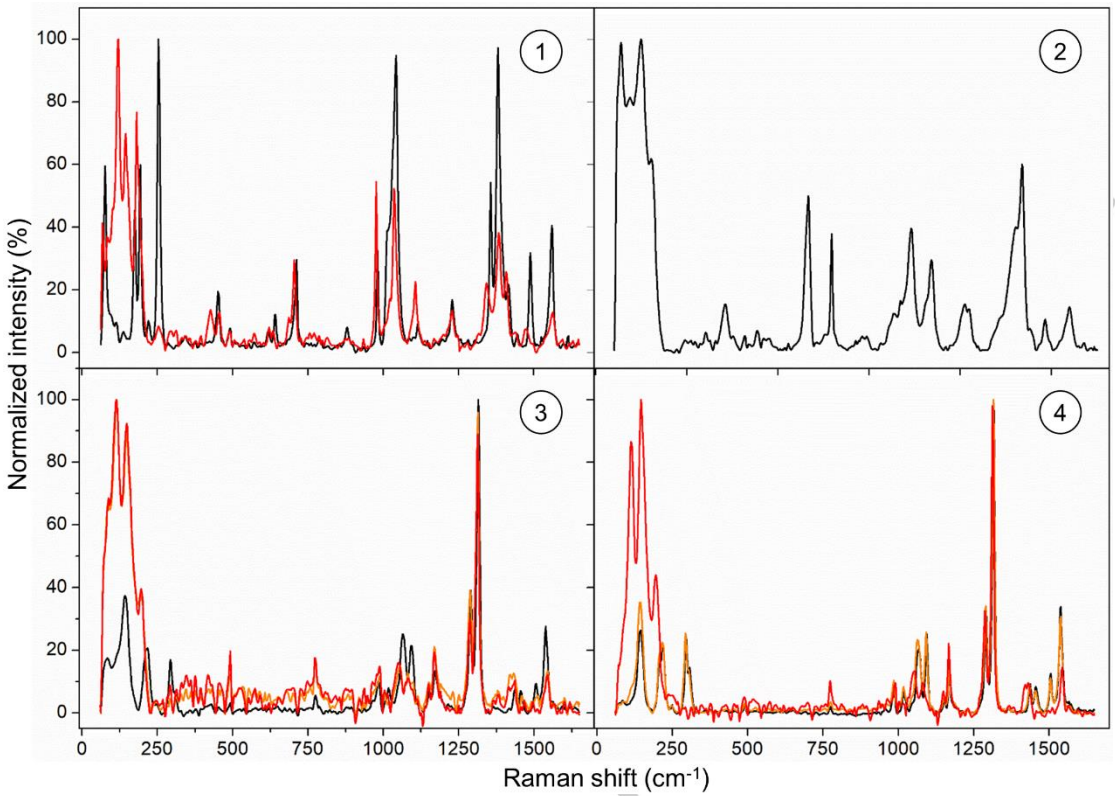

Figure 6. Raman spectra of **1–4** measured in the 298–393 K range. Excitation wavelength 532 nm. Red line – 393 K, orange line – 363 K, black line – 298 K

and LS states reveal typical changes in the spectrum associated with SCO[51].

The spectra of all the investigated compounds in the LS state show three bands in the region of 200–300 cm^{-1} that can be safely attributed to Fe–N stretching mode. These bands become more intensive and closer to each other with the transition to the HS state and therefore can be used as marker bands of spin transition. For all compounds, such changes of bands upon SCO can be explained by elongation and weakening of Fe–N bonds and symmetry lifting for $[FeN_6]$ coordination environment.

For complex **1** two Raman spectra were recorded: at 298 K where the complex is in the LS state and at 393 K where complex is in the HS state. In HS two peaks at 426 and 455 cm^{-1}, two peaks at 621 and 634 cm^{-1} and a peak at 977 cm^{-1} can be tentatively attributed to the $v_2(E)$, $v_4(F_2)$ and $v_1(A_1)$ vibration modes of SO_4^{2-}, respectively.[52] In the LS state vibrations of SO_4^{2-} can be observed at 452 cm^{-1}, 621 cm^{-1}, 641 cm^{-1} and 981 cm^{-1}. Three bands at 174, 193 and 254 cm^{-1} in LS state can be safely attributed to Fe–ligand stretching vibrations. Upon transition to HS state, these bands undergo red shift and can be observed at 120, 144 and 181 cm^{-1}. Band at 712 cm^{-1} in LS form can be safely assigned to N–NH_2 stretching vibrations. This band is insignificantly red shifted upon transition to HS state and can be observed at 705 cm^{-1}.

The band in **2** at 777 cm^{-1} can be safely assigned to the totally symmetric stretching vibrations of the BF_4^-. The three bands at 83, 112, 151 cm^{-1} are more likely assigned to Fe–ligand stretching vibrations. A more detailed description of Raman spectra of **1** and **2** is given in SI.

The Raman spectra of **3** and **4** are very similar as these samples are two modifications of the complex $[Fe(Htrz)_2(trz)]BF_4$. For these modifications three Raman spectra were recorded at different temperatures: at 298, 363, 393 K. For **3** (for which spin transition temperature is centered at 343 K) Raman spectrum at 363 K indicates that the complex is in the HS state, at the same time **4** is still LS at this temperature. The most interesting changes can be observed in low frequency region below 400 cm^{-1}. The three bands at 143, 213, 298 cm^{-1} can be found for the LS form of these complexes. These bands can be safely assigned to Fe–ligand stretching vibrations. Upon heating these bands are shifted towards low frequencies and three bands at 113, 146, 195 cm^{-1} for the HS state can be observed. For **3** the bands at 1068 and 1315 cm^{-1} for the LS state as well as the bands at 1051 and 1312 cm^{-1} for HS state are characteristic for *Htrz*. At the same time, the bands at 1094 and 1291 cm^{-1} for LS state as well as the bands at 1081 and 1288 cm^{-1} for the HS state are characteristic for *trz*. The rough ratio of the area under the band at 1291 cm^{-1} (*trz*) to the area under the band at 1315 cm^{-1} (*Htrz*) is 1:2. This confirms that the stoichiometry of *trz* and *Htrz* in **3** is 1:2. The same trend is observed for **4** although the position of the characteristic bands is slightly different compared to the **3**.

Conclusion

We show a novel method to synthesize SCO active compounds by “direct synthesis”. Four different complexes of iron(II) with 4-R-1,2,4-triazoles were obtained by this approach.

A high degree of crystallinity of $[Fe(NH_2trz)_3]SO_4$ complex allowed to obtain its crystal structure by Rietveld refinement of a PXRD pattern. It was concluded that $[Fe(NH_2trz)_3]SO_4$ crystalizes in $P6_3/m$ space group. The 1D polymeric structure of $[Fe(NH_2trz)_3]SO_4$ consist of infinite $[Fe(NH_2trz)]_n$ chains that are connected through N–H···O hydrogen bonds and anion···π interactions. Importantly, the quality of PXRD pattern of

$[Fe(NH_2trz)_3]SO_4$ does not depend on synthetic approach that was applied.

All the SCO characteristics of the complexes, namely temperature, abruptness and completeness of spin transition, obtained by direct synthesis are retained. Additionally, the possibility to obtain different modifications of one complex by direct synthesis approach was shown. We believe that this work will provide a starting point for obtaining new SCO complexes by direct synthesis which are unavailable via more classical approaches.

Experimental Section

Synthesis. Powder samples **1–4** were obtained by direct synthesis approach by mixing iron powder, ligand, anion containing salts and minor quantity of acid in corresponding solvents (the exact quantities of precursors are given in Table 3). Mixtures were stirred for one week. During the flow of the reaction the formation of SCO complex (purple for **1**, **3**, **4** and white for **2)** is observed. After that the mixture was easily purified from metallic iron by attracting the leftovers with NdFeB magnet. The precipitate was separated from the solvent by centrifugation (950 RPM for about 3 min), washed with corresponding solvent (4 times × 2 ml of solvent, stirred for 5 min), then centrifuged (950 RPM, 3 min × 4 times) and dried on air. The excess of corresponding ligand was added to ensure the inclusion of only corresponding ligand into complex. IR spectra of **1–4** are given in Figures S6–9.

Powder samples of the same complexes, which were obtained by conventional method for the comparison of PXRD patterns, were synthesized as follows:

$[Fe(NH_2trz)_3]SO_4$. A solution of 103 mg (1.24 mmol) of 4-amino-1,2,4-triazole in 1.5 ml of methanol at 60 °C was added to a solution of 69 mg (0.25 mmol) of $FeSO_4·7H_2O$ in 0.5 ml of water at 60 °C and then 10 µl H_2SO_4 were added in order to facilitate the dissolution of iron and prevent the oxidation of Fe^{II} to Fe^{III} during the synthesis (excess of ligand was used to ensure the inclusion of only corresponding ligand into complex). A purple precipitate appeared after a short while. Then the reaction mixture was cooled and kept at 5 °C for 5 h. After that the precipitate was separated from the solvent by centrifugation (950 RPM, 3 min × 3 times), washed with methanol (3 times × 2 ml of methanol, stirred for 5 min), then centrifuged (950 RPM, 3 min × 3 times) and dried on air. The complex was synthesized according to Lavrenova at al.[34] Elemental analysis of $C_6H_{12}SO_4Fe$: calc. C, 17.83; H, 2.99; N, 41.59; O, 15.84; S, 7.93; found C, 17.78; H, 2.92; N, 41.55; O, 15.86; S, 7.96%. Yield: 73%.

$[Fe(NH_2trz)_3](BF_4)_2$. A solution of 98 mg (1.17 mmol) of 4-amino-1,2,4-triazole in 1.5 ml of ethanol was added to a solution of 79 mg (0.23 mmol) of $Fe(BF_4)_2·6H_2O$ in 5 ml of ethanol (excess of ligand was used to ensure the inclusion of only corresponding ligand into complex). A precipitate appeared after a short while; its color was first white and then turned to pink. Then the reaction mixture was cooled and kept at 5 °C for 5 h. The precipitate was separated from the solvent by centrifugation (950 RPM, 3 min × 3 times), washed with ethanol (3 times × 2 ml of ethanol, stirred for 5 min), then centrifuged (950 RPM, 3 min × 3 times) and dried on air. The complex was synthesized according to Lavrenova at al.[34] Elemental analysis of $C_6H_{12}B_2F_8Fe$: calcd. C, 14.96; H, 2.51; N, 34.89; found C, 14.91; H, 2.45; N, 34.84%. Yield: 83%.

$[Fe(NH_2trz)_3](BF_4)_2$. A solution of 98 mg (1.17 mmol) of 4-amino-1,2,4-triazole in 1.5 ml of ethanol was added to a solution of 79 mg (0.23 mmol) of $Fe(BF_4)_2·6H_2O$ in 5 ml of ethanol (excess of ligand was used to ensure the inclusion of only corresponding ligand into complex). A precipitate appeared after a short while; its color was first white and then turned to pink. Then the reaction mixture was cooled and kept at 5 °C for 5 h. The precipitate was separated from the solvent by centrifugation (950 RPM, 3 min × 3 times), washed with ethanol (3 times × 2 ml of ethanol, stirred for 5 min), then centrifuged (950 RPM, 3 min × 3 times) and dried on air. The complex was synthesized according to Lavrenova at al.[34] Elemental analysis of $C_6H_{12}B_2F_8Fe$: calcd. C, 14.96; H, 2.51; N, 34.89; found C, 14.91; H, 2.45; N, 34.84%. Yield: 83%.

$[Fe(trz)(Htrz)_2]BF_4$ (Ib). A solution of 119 mg (1.72 mmol) of 1H-1,2,4-triazole in 0.57 ml of methanol was added to a solution of 193 mg (0.57 mmol) of $Fe(BF_4)_2·6H_2O$ in 3 ml of methanol (excess of ligand was used to ensure the inclusion of only corresponding ligand into complex). A precipitate appeared after a short while; its color was first white and then turned to pink. Then the reaction mixture was cooled and kept at 5 °C for 5 h. The precipitate was separated from the solvent by centrifugation (950 RPM, 3 min × 3 times), washed with methanol (3 times × 2 ml of methanol, stirred for 5 min), then centrifuged (950 RPM, 3 min × 3 times) and dried on air. The complex was synthesized according to Kröber at al.[35] Elemental analysis of $C_6H_8BF_4Fe$: calcd. C, 20.66; H, 2.31; N, 36.14; found C, 20.64; H, 2.28; N, 36.1%. Yield: 81.5%.

CHN. Elemental analyses were performed with a Vario Micro Cube (Elemental) CHNOS elemental analyzer.

Magnetic susceptibility measurements. Magnetic susceptibilities were measured in the temperature range 300 - 390 K for **1**, 75 – 250 K for **2**, and 300 – 400 K for **3** and **4** using MPMS-XL (7T) SQUID magnetometer.

Table 3. Synthesis.

Sample	1	2	3	4
Iron	0.028 g; $5·10^{-4}$ mol	0.02 g; $3.57·10^{-4}$ mol	0.032 g; $5.71·10^{-4}$ mol	0.02 g; $3.57·10^{-4}$ mol
Ligand	NH_2trz (0.6 g; $7.14·10^{-3}$ mol)	NH_2trz (0.45 g; $5.36·10^{-3}$ mol)	Htrz (0.6 g; $8.7·10^{-3}$ mol)	Htrz (0.37 g; $5.36·10^{-3}$ mol)
Salt	$(NH_4)_2SO_4$ (0.066 g; $5·10^{-4}$ mol)	$NaBF_4$ (0.082 g; $7.45·10^{-4}$ mol)	$NaBF_4$ (0.063 g; $5.71·10^{-4}$ mol)	$NaBF_4$ (0,039 g; $3.57·10^{-4}$ mol)
Acid	H_2SO_4 (96 %) (10 µl)	HBF_4 (48 %) (0.1 ml)	HBF_4 (48 %) (0.1 ml)	HBF_4 (48 %) (0.1 ml)
Solvent	Methanol (1.5 ml) H_2O (0.5 ml)	Ethanol (2 ml)	Acetonitrile (2 ml)	Methanol (2 ml)
CHN calc.	C, 17.83; H, 2.99; N, 41.59; O, 15.84; S, 7.93	C, 14.96; H, 2.51; N, 34.89;	C, 20.66; H, 2.31; N, 36.14;	C, 20.66; H, 2.31; N, 36.14;
CHN found	C, 17.79; H, 3.01; N, 42.63; O, 15.82; S, 7.91%	C, 14.99; H, 2.48; N, 34.85;	C, 20.68; H, 2.28; N, 36.07;	C, 20.69; H, 2.30; N, 36.09;
Yield	59 %	85 %	82 %	73 %
Color (298 K)	purple	white	purple	purple

Cooling and heating rates were 3 K min^{-1}, magnetic field was 0.1 T. Diamagnetic correction was applied using Pascal's constants.

Optical measurements. The optical reflectivity measurements were conducted using optical microscope Optica SZM-1 equipped with a Sigeta UCMOS 1300 camera. The sample temperature was controlled with a Linkam DSC600 cryostat operating at 5 K min^{-1} heating/cooling rates. Before each experiment the stage chamber was purged with dry nitrogen for about 5 minutes. Photographs were taken automatically using ToupView software (1 image per K). The images analysis was performed with ImageJ software. The image array was splitted into channels. Further, image processing was performed in green channel.

DSC measurements. Differential scanning calorimetry measurements were carried out using a Linkam DSC600 calorimeter. Heating/cooling rate was 10 K min^{-1}. Before each experiment the stage chamber was purged with dry nitrogen for 5 minutes.

Raman spectroscopy. Raman spectra were recorded using Horiba Scientific LabRam HR Evolution spectrometer. The 532 nm laser was used for excitation. Temperature control was realized using Linkam THMS 600 cryostat.

FTIR. IR spectra were recorded on preheated samples in Nujol using Perkin Elmer SPECTRUM BX II FT-IR System.

Powder X-ray diffraction and Rietveld refinement. The PXRD pattern was acquired on Shimadzu XRD-6000 diffractometer using Cu-Kα radiation (5-50 ° range, 0.02° step, 6s acquisition). Indexing of the powder pattern was done with N-TREOR09 software.[53] Initial model of the structure was built with EXPO2014[54] software using a simulated annealing approach. The $P6_3/m$ symmetry of the compound was deduced from the statistics of the normalized intensities and the same group was suggested for the annealed structure by Platon.[55] The model was refined with GSAS II[56] by Rietveld Refinement method with all atoms treated isotopically. Chebyschev function with 10 terms was used to fit the background. Gaussian function was used to model the peak shape. Crystallite size was modeled as isotropic. Bond distances were constrained. The Fe-(NH_2trz) moiety was constrained to lay in the plane. O-S-O angle was constrained. U_{iso} of all non-H atoms were restrained to be the same and refined simultaneously. Hydrogen atoms were placed at calculated positions with $U_{iso}(H)= 1.2\ U_{iso}(C,N)$. The R_{wp} and R_p values are listed in Table 1. CCDC 2016284.

Acknowledgements

This project has received funding from the European Union's Horizon 2020 research and innovation programme under the Marie Skłodowska-Curie grant agreement No 734322 and Ministry of Education and Science of Ukraine (grants No. 19BF037-01M and 19BF037-04).

Keywords: spin crossover • direct synthesis • Fe(II) coordination compounds • triazoles • crystal structure

[1] P. Gütlich, H. A. Goodwin, Eds. , *Spin Crossover in Transition Metal Compounds I*, Springer Berlin Heidelberg, Berlin, Heidelberg, **2004**.

[2] A. Hauser, in *Spin Crossover Transit. Met. Compd. I* (Eds.: P. Gütlich, H.A. Goodwin), Springer-Verlag: Berlin/Heidelberg, **2004**, pp. 49–58.

[3] H. J. Shepherd, I. A. Gural'skiy, C. M. Quintero, S. Tricard, L. Salmon, G. Molnár, A. Bousseksou, *Nat. Commun.* **2013**, *4*, 2607.

[4] A. Rotaru, J. Dugay, R. P. Tan, I. A. Guralskiy, L. Salmon, P. Demont, J. Carrey, G. Molnár, M. Respaud, A. Bousseksou, *Adv. Mater.* **2013**, *25*, 1745–1749.

[5] A. Rotaru, I. A. Gural'skiy, G. Molnár, L. Salmon, P. Demont, A. Bousseksou, *Chem. Commun.* **2012**, *48*, 4163.

[6] M. Ohba, K. Yoneda, G. Agustí, M. Carmen Muñoz, A. B. Gaspar, J. A. Real, M. Yamasaki, H. Ando, Y. Nakao, S. Sakaki, et al., *Angew. Chemie Int. Ed.* **2009**, *48*, 4767–4771.

[7] R. Ohtani, S. Hayami, *Chem. - A Eur. J.* **2017**, *23*, 2236–2248.

[8] I. A. Gural'skiy, S. I. Shylin, V. Ksenofontov, W. Tremel, *Eur. J. Inorg. Chem.* **2017**, *2017*, 3125–3131.

[9] O. I. Kucheriv, V. V. Oliynyk, V. V. Zagorodnii, V. L. Launets, I. A. Gural'skiy, *Sci. Rep.* **2016**, *6*, 38334.

[10] O. Kahn, C. J. Martinez, *Science (80-.).* **1998**, *279*, 44–48.

[11] L. Salmon, G. Molnár, D. Zitouni, C. Quintero, C. Bergaud, J.-C. J.-C. C. Micheau, A. Bousseksou, *J. Mater. Chem.* **2010**, *20*, 5499–5503.

[12] K. Senthil Kumar, M. Ruben, *Coord. Chem. Rev.* **2017**, *346*, 176–205.

[13] J. H. Askew, H. J. Shepherd, *Chem. Commun.* **2018**, *54*, 180–183.

[14] J. Li, Z. Chen, R.-J. Wang, D. M. Proserpio, *Coord. Chem. Rev.* **1999**, *190–192*, 707–735.

[15] P. Köse Yaman, H. Erer, M. Arıcı, İ. Eruçar, O. Z. Yeşilel, *Inorganica Chim. Acta* **2019**, *488*, 229–237.

[16] E. C. Ellingsworth, B. Turner, G. Szulczewski, *RSC Adv.* **2013**, *3*, 3745.

[17] X.-B. Fan, S. Yu, H.-L. Wu, Z.-J. Li, Y.-J. Gao, X.-B. Li, L.-P. Zhang, C.-H. Tung, L.-Z. Wu, *J. Mater. Chem. A* **2018**, *6*, 16328–16332.

[18] V. C. Chandrashekhar, B. M. Muñoz Flores, V. M. Jiménez-Pérez, in *Direct Synth. Met. Complexes*, **2018**, pp. 25–85.

[19] B. Gerdes, *J. für Prakt. Chemie* **1882**, *26*, 257–276.

[20] S. Fedrigo, T. L. Haslett, M. Moskovits, *J. Am. Chem. Soc.* **1996**, *118*, 5083–5085.

[21] M. N. Temnikov, A. A. Anisimov, P. V. Zhemchugov, D. N. Kholodkov, A. S. Goloveshkin, A. V. Naumkin, S. M. Chistovalov, D. Katsoulis, A. M. Muzafarov, *Green Chem.* **2018**, *20*, 1962–1969.

[22] Y. I. Slyvka, B. M. Mykhalichko, E. A. Goreshnik, V. N. Davydov, *Russ. J. Inorg. Chem.* **2007**, *52*, 165–171.

[23] B. I. Kharisov, D. A. Garnovskii, L. M. Blanco, A. S. Burlov, I. S. Vasilchenko, A. D. Garnovskii, *Polyhedron* **1999**, *18*, 985–988.

[24] V. N. Kokozay, O. Y. Vassilyeva, P. Weinberger, M. Wasinger, W. Linert, *Rev. Inorg. Chem.* **2000**, *20*, 255–282.

[25] B. Liu, Q. Xia, W. Chen, *Angew. Chemie* **2009**, *121*, 5621–5624.

[26] S. Schlecht, *Angew. Chemie Int. Ed.* **2002**, *41*, 1178–1180.

[27] E. G. Rochow, *J. Chem. Educ.* **1966**, *43*, 58–62.

[28] D. S. Nesterov, O. V. Nesterova, V. N. Kokozay, A. J. L. Pombeiro, *Eur. J. Inorg. Chem.* **2014**, *2014*, 4496–4517.

[29] A. D. Garnovskii, B. I. Kharisov, G. Gojon-Zorrilla, D. A. Garnovskii, *Russ. Chem. Rev.* **1995**, *64*, 201–221.

[30] O. Roubeau, J. M. Alcazar Gomez, E. Balskus, J. J. A. Kolnaar, J. G. Haasnoot, J. Reedijk, *New J. Chem.* **2001**, *25*, 144–150.

[31] I. A. Gural'skiy, V. A. Reshetnikov, A. Szebesczyk, E. Gumienna-Kontecka, A. I. Marynin, S. I. Shylin, V. Ksenofontov, I. O. Fritsky, *J. Mater. Chem. C* **2015**, *3*, 4737–4741.

[32] O. Roubeau, *Chem. - A Eur. J.* **2012**, *18*, 15230–15244.

[33] I. A. Gural'skiy, O. I. Kucheriv, S. I. Shylin, V. Ksenofontov, R. A. Polunin, I. O. Fritsky, *Chem. - A Eur. J.* **2015**, *21*, 18076–18079.

[34] L. G. Lavrenova, O. G. Shakirova, V. N. Ikorskii, V. A. Varnek, L. A.

Sheludyakova, S. V Larionov, *Russ. J. Coord. Chem.* **2003**, *29*, 22–27.

[35] J. Kroeber, J.-P. Audiere, R. Claude, E. Codjovi, O. Kahn, J. G. Haasnoot, F. Groliere, C. Jay, A. Bousseksou, *Chem. Mater.* **1994**, *6*, 1404–1412.

[36] L. G. Lavrenova, V. N. Ikorskii, V. A. Varnek, I. M. Oglezneva, S. V. Larionov, *Koord. Khim.* **1990**, *16*, 654–661.

[37] B. Dreyer, D. Natke, S. Klimke, S. Baskas, R. Sindelar, G. Klingelhöfer, F. Renz, *Hyperfine Interact.* **2018**, *239*, 2–9.

[38] A. Lapresta-Fernández, S. Titos-Padilla, J. M. Herrera, A. Salinas-Castillo, E. Colacio, L. F. Capitán Vallvey, *Chem. Commun.* **2013**, *49*, 288–290.

[39] A. Lapresta-Fernández, M. P. Cuéllar, J. M. Herrera, A. Salinas-Castillo, M. D. C. Pegalajar, S. Titos-Padilla, E. Colacio, L. F. Capitán-Vallvey, *J. Mater. Chem. C* **2014**, *2*, 7292–7303.

[40] D. Onggo, in *AIP Conf. Proc.*, **2014**, pp. 272–275.

[41] A. Grosjean, N. Daro, B. Kauffmann, A. Kaiba, J.-F. Létard, P. Guionneau, *Chem. Commun.* **2011**, *47*, 12382.

[42] N. Pittala, F. Thétiot, S. Triki, K. Boukheddaden, G. Chastanet, M. Marchivie, *Chem. Mater.* **2017**, *29*, 490–494.

[43] A. Grosjean, P. Négrier, P. Bordet, C. Etrillard, D. Mondieig, S. Pechev, E. Lebraud, J.-F. Létard, P. Guionneau, *Eur. J. Inorg. Chem.* **2013**, *2013*, 796–802.

[44] A. Urakawa, W. Van Beek, M. Monrabal-Capilla, J. R. Galán-Mascarós, L. Palin, M. Milanesio, *J. Phys. Chem. C* **2011**, *115*, 1323–1329.

[45] L. G. Lavrenova, O. G. Shakirova, *Eur. J. Inorg. Chem.* **2013**, 670–682.

[46] I. A. Gural'skiy, P. V Solntsev, H. Krautscheid, K. V Domasevitch, *Chem. Commun.* **2006**, 4808–4810.

[47] N. G. White, J. A. Kitchen, S. Brooker, *Eur. J. Inorg. Chem.* **2009**, 1172–1180.

[48] G. A. Senchyk, A. B. Lysenko, D. Y. Naumov, V. P. Fedin, H. Krautscheid, K. V. Domasevitch, *Inorg. Chem. Commun.* **2010**, *13*, 1576–1579.

[49] J. Tao, R. J. Wei, R. Bin Huang, L. S. Zheng, *Chem. Soc. Rev.* **2012**, *41*, 703–737.

[50] O. Roubeau, M. Castro, R. Burriel, J. G. Haasnoot, J. Reedijk, *J. Phys. Chem. B* **2011**, *115*, 3003–3012.

[51] J. A. Wolny, R. Diller, V. Schünemann, *Eur. J. Inorg. Chem.* **2012**, *2012*, 2635–2648.

[52] K. Ben Mabrouk, T. H. Kauffmann, H. Aroui, M. D. Fontana, *J. Raman Spectrosc.* **2013**, *44*, 1603–1608.

[53] P. E. Werner, L. Eriksson, M. Westdahl, *J. Appl. Crystallogr.* **1985**, *18*, 367–370.

[54] A. Altomare, C. Cuocci, C. Giacovazzo, A. Moliterni, R. Rizzi, N. Corriero, A. Falcicchio, *J. Appl. Crystallogr.* **2013**, *46*, 1231–1235.

[55] A. L. Spek, *Acta Crystallogr. Sect. D Biol. Crystallogr.* **2009**, *65*, 148–155.

[56] B. H. Toby, R. B. Von Dreele, *J. Appl. Crystallogr.* **2013**, *46*, 544–549.

Entry for the Table of Contents

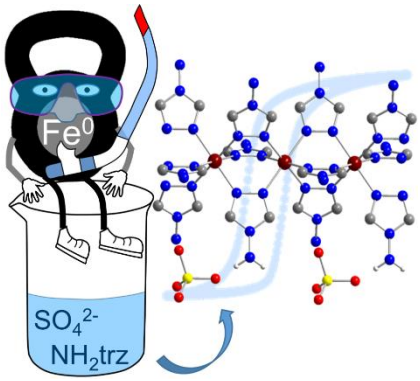

Here we propose a direct synthesis approach for obtaining spin-crossover materials from metallic iron. According to this route, four Fe^{II} based complexes with 4-R-1,2,4-triazole have been synthesized and thoroughly characterized. In addition, by performing Rietveld refinement we managed to obtain a crystal structure of $[Fe(NH_2trz)_3]SO_4$ complex revealing its 1D polymeric architecture.

Key Topic: Spin-Crossover Complexes